Published in final edited form as:
Liedel, C., Wang, X., & Antonietti, M. (2018). Biobased polymer cathodes with enhanced charge storage. Nano Energy, 53, 536-543. doi:10.1016/j.nanoen.2018.09.012.

Biobased polymer cathodes with enhanced charge storage

Clemens Liedel, Xuewan Wang, and Markus Antonietti

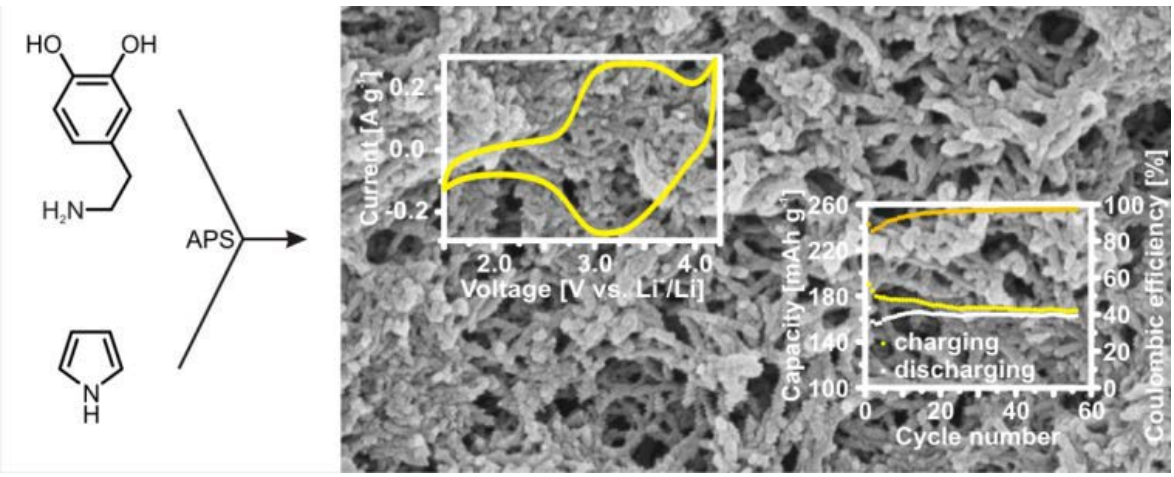

Highlights
- Dopmine and pyrrole form a copolymer with nanofibrille structure
- Charge storage is a synergistic and enhanced combination of both constituents
- The resulting material might be used as cathode in organic batteries

Biobased Polymer Cathodes with Enhanced Charge Storage

Clemens Liedel,* Xuewan Wang, and Markus Antonietti

Department of Colloid Chemistry, Max Planck Institute of Colloids and Interfaces, Research Campus Golm, Am Mühlenberg 1, 14476 Potsdam, Germany

E-mail: Clemens.Liedel@mpikg.mpg.de

Electronic Supplementary Information (ESI) attached: sketch about the synthesis procedure, UV-Vis, TGA, FT-IR, capacity of different Ppy-DA_x compositions.

While increasing worldwide energy consumption demands for better storage devices, the environmental impact of these is often neglected. More sustainable energy storage in terms of greener battery materials would be desirable. In this regard, bioderived quinone containing molecules may serve as active battery material. Here, dopamine, among others an important neurotransmitter or active in mussel adhesion, is copolymerized with pyrrole to form a rod-like mixed copolymer. n-type charge storage in the quinone functionalities is combined with p-type charge storage in the conjugated doped polymer backbone from pyrrole and dopamine units with decreased polaron delocalization length compared to neat polypyrrole. The resulting sustainable polymer can be used as a cathode material due to a favorable redox potential of approx. 3.0-3.5 V vs. Li^+/Li. It can reversibly store 160 mAh g^{-1} at a discharging rate of 100 mA g^{-1} and hence achieve similar capacities than inorganic, unsustainable, cathode materials and significantly higher capacities than other sustainable cathodes. Capacity is stable for more than 50 cycles, and even at high discharging rate of 800 mA g^{-1}, approximately 90 mAh g^{-1} are reversibly stored with coulombic efficiency of almost 100 %.

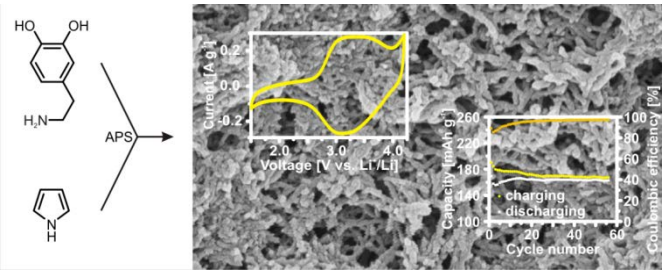

Keywords: dopamine, nanofibrille, organic battery, charge storage, copolymer, sustainable chemistry

Highlights

- Dopmine and pyrrole form a copolymer with nanofibrille structure

- Charge storage is a synergistic and enhanced combination of both constituents

- The resulting material might be used as cathode in organic batteries

1. Introduction

Modern society would be unthinkable without achievements in energy storage in the form of lithium ion batteries (LIBs). Still, the worldwide hunger for even better batteries in terms of higher charge storage capacity or higher energy density is strong. Consequently, mining of metals like lithium or cobalt, required for fabricating LIBs, has been strongly expanded, resulting in a competition for resources with the known environmental and socioeconomic side effects. Additionally, more and more batteries end up in landfill waste. All of this inherently implies ecological and social concerns.[1, 2]

More sustainable batteries have been investigated[3] which include non-lithium technologies like batteries based on sodium,[4] magnesium,[5] aluminum[6], or organic species[7] on the anode side as well as sulfur-,[8] air-,[9] and organic systems on the cathode side.[10] Organic cathode systems have the advantage that they replace the critical cobalt completely. Designer polymers or covalent organic frameworks with quinone functionalities have been presented as cathodes for future batteries with high charge storage of significantly more than 200 mAh g^{-1}.[11, 12] Even more important, organic cathodes may be produced from regrowing biomass, therefore being fully sustainable and definitely less toxic.[13, 14] In this regard, biomolecules with quinone or hydroquinone motifs are attractive as electroactive species.[15]

One especially interesting compound is polydopamine (PDA), as it can easily be polymerized from the biomolecule dopamine and – even though the structure is not fully understood – contains a quinone or hydroquinone functionality in every repeating unit.[16] Polydopamine is definitely biocompatible, as for instance the black pigments in human hair or the color of black bird feathers is due to nanostructures of polydopamine.[17] Polydopamine itself is not sufficiently conductive, so a combination with a conductive additive is crucial for using its redox activity for charge storage applications. Recently it has been presented as an organic electrode material upon polymerization onto carbon nanotubes.[18] The nanotubes not only provide the conductivity in the system but act also as electroactive material by capacitive charge storage.

Besides the still high price of carbon nanotubes, unclear properties regarding health and safety may limit applicability of this approach.[19] An alternative option to increase conductivity and to use synergistic charge storage properties in organic electrode materials preferred by us is to combine dopamine chemistry with conductive polymers.[20] In this regard, increased conductivity and good adhesive properties have been reported when

dopamine is copolymerized with pyrrole.[21, 22] While the exact structure is again not fully resolved, both monomers are covalently connected by incorporation of dopamine into the polypyrrole (PPy) chain[21] while hydrogen bonding and π-stacking of aromatic units of dopamine and pyrrole promotes interchain charge transport.[23] Particularly, applications of such copolymers as biosensor or biocompatible adhesion promoter, e.g., for bone implants, have been described.[21, 22, 24] Because of their good electric properties, they have also been tested in supercapacitor applications.[25]

For energy storage applications, incorporation of a conjugated polymer into the cathode has the advantage of additional charge storage by polaron formation within the p-type polymer, together with n-type charge storage in the quinone-hydroquinone redox couple. Usually, however, the polaron delocalization length, i.e., the distance between charges in a conjugated polymer, is rather long and depends amongst others on molecular order, crystallinity, and electron-lattice coupling.[26, 27] For energy storage applications, decreased polaron delocalization length would be advantageous.

In addition to the known good conductivity and adhesion,[21, 22] pyrrole-dopamine copolymers are supposed to have a high density of quinone functionalities and the possibility of charge storage in the conjugated backbone. This makes such copolymers promising candidates for more sustainable cathodes in rechargeable lithium (or sodium, magnesium,…) batteries.

Still, battery cathode applications of pyrrole-dopamine copolymers have not been presented to the best of our knowledge. Together with discussions regarding the structure, herein we present the charge storage properties of pyrrole-dopamine copolymers as cathode material in rechargeable lithium batteries.

2. Materials and Methods

2.1. Synthesis of PPy-DA copolymers

The synthesis of PPy-DA_1 is described as an example; samples with different dopamine-to-pyrrole ratio were prepared accordingly. First, pyrrole monomer (0.116 g, 1.73 mmol) and dopamine hydrochloride (0.328 g, 1.73 mmol, 1 eq) were added to 25 mL Tris-HCl buffer solution (pH = 8.5, 10 mM) followed by continuous magnetic stirring for 5 min to form a homogenous solution. Subsequently, the solution was cooled down to 8 °C in a circulating water bath. Under vigorous stirring, ammonium persulfate (0.5 g, 2.19 mmol, 1.27 eq in 5 mL Tris-HCl buffer solution) was then slowly added. The mixture was maintained at the same condition for 18 h. The precipitate was collected from the resulting dark green solution by centrifugation, washed with deionized water 4 times and then with ethanol 2 times. The product was dried at 60 °C in vacuum, resulting in a black solid.

2.2. Analysis

UV-Vis spectroscopy was carried out using a PG Instruments Ltd. T70+ Spectrometer. Scanning electron microscopy (SEM) images were taken using a Zeiss Leo Gemini 1550 microscope. Fourier transform infrared (FT-IR) spectroscopy was measured using a Nicolet iS

5 FT-IR spectrometer with an attenuated total reflection unit. Elemental composition was investigated by combustion analysis using a Vario Micro device. Thermogravimetric analysis (TGA) was performed on a Netzsch TG 209 F1 Libra in nitrogen atmosphere with a heating rate of 10 K min^{-1}. Cyclic voltammetry (CV) and galvanostatic charging-discharging measurements were performed using a BioLogic MPG2 potentiostat in self-made 2-electrode Swagelok®-type cells using 1 M $LiPF_6$ in EC/DMC (1:1; v:v) as electrolyte and lithium foil as counter electrode. The active material, blended with acetylene black (EQ-Lib-AB, MTI) and PVDF (6:3:1; w:w:w) and coated on a graphite sheet current collector (kindly donated by Henschke GmbH, Germany) with a loading in the range of 2 mg cm^{-2}, served as cathode.

3. Results and Discussion

3.1. Dopamine-Pyrrole Copolymers

We polymerized pyrrole in the presence of dopamine at 8 °C by oxidative polymerization using ammonium persulfate (APS) as initiator (cf. Figure 1, Experimental Section, and Figure S1). The feeding ratio of dopamine to pyrrole was varied from 0.16:1 to 1:1. Additionally, samples without the one or the other monomer were prepared. Samples are consequently denoted PPy, PDA, PPy-$DA_{0.16}$, PPy-$DA_{0.32}$, and PPy-DA_1, with the index denoting the dopamine-to-pyrrole ratio.

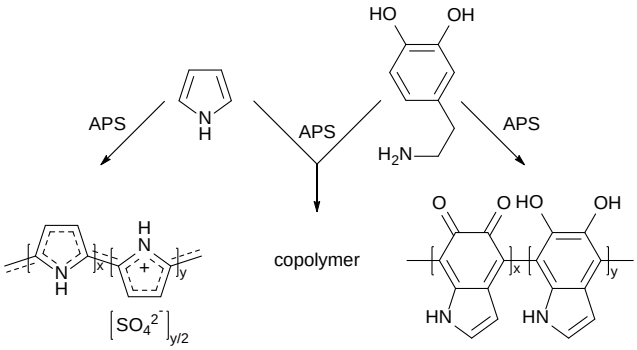

Fig. 1 Schematics of the oxidative polymerization of pyrrole (left), a mixture of pyrrole and dopamine (middle), and dopamine (right) with ammonium persulfate showing idealized structures.

Already few seconds after addition of the oxidant, solutions change color and become increasingly dark. Notably, this change of color is fastest for reactions in which both pyrrole and dopamine are present. Solutions which contain only one monomer take significantly longer, and both the color and the consistency of the solutions/dispersions differ. This is illustrated in Figure 2a-c. Dopamine forms a slightly colored solution from the beginning, turns red upon addition of the oxidant, and becomes darker red with prolonged reaction. A very fine precipitate is formed. Pyrrole in contrast is colorless in solution and more quickly turns dark upon addition of the oxidant with a black precipitate forming. A 1:1 mixture of dopamine and pyrrole turns dark fastest after addition of the oxidant, and a fine precipitate

forms in a greenish solution. This precipitate can be separated from the solution in the form of a fine black powder. All precipitates are unsoluble in any solvent investigated, which inhibits determination of molecular weights of the formed polymers.

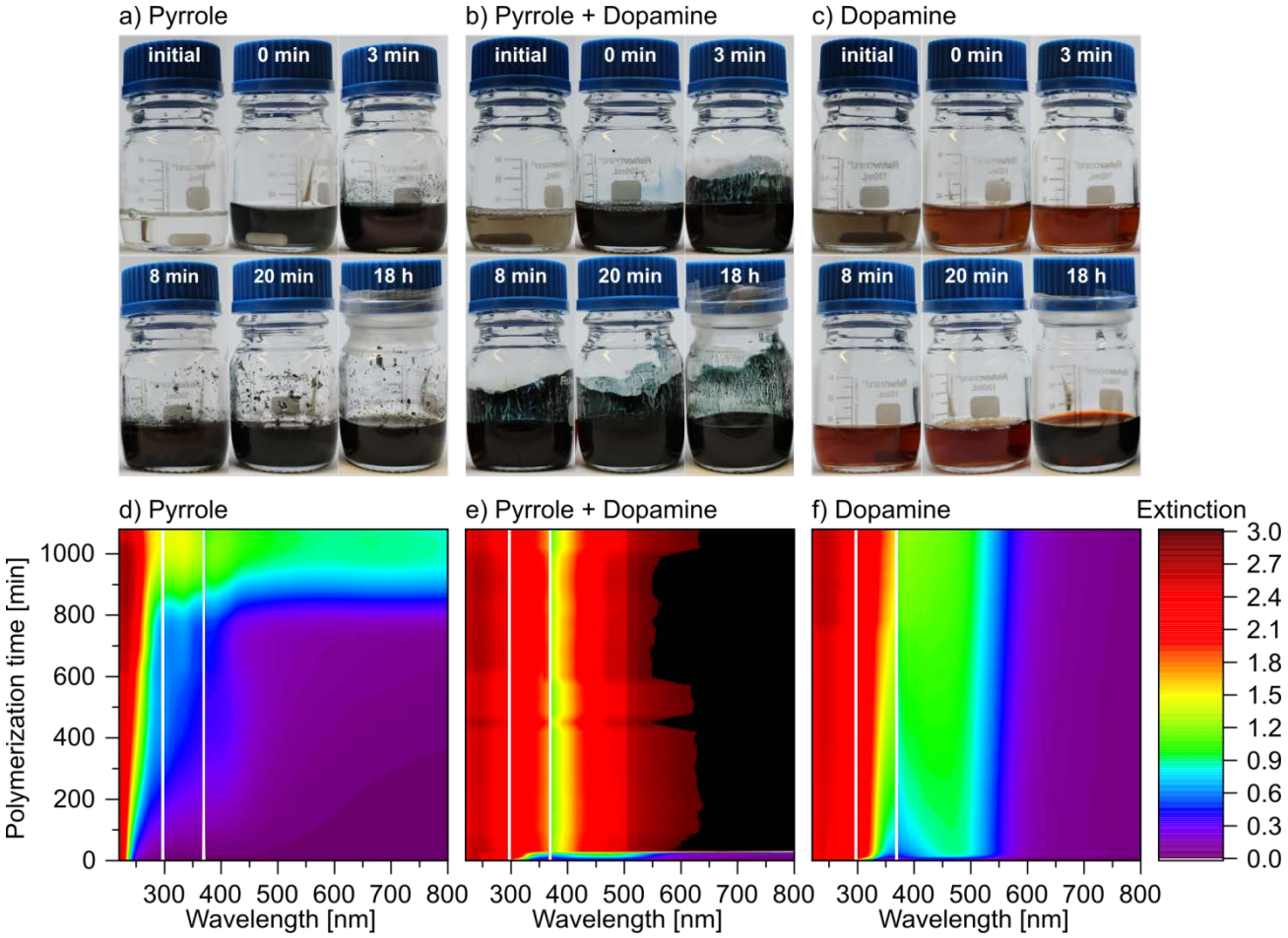

Fig. 2 Optical characterization of the polymerization of PPy, PPy-DA_1, and PDA. a-c) Photographs show the solutions before addition of the oxidant and with increasing reaction time as indicated. d-f) In-situ UV-Vis spectroscopy shows the change of extinction with time. Polymerization was performed in diluted solution (1:10) to slow down the kinetics. Missing wavelengths (white) are caused by different detectors and detector failures. Areas colored yellow, orange and higher spectrum exceed the limits of the Beer-Lambert law. Photographs of the reaction mixtures from (d-f) after the polymerization (Figure S9) resemble the ones of (a-c).

In-situ UV-Vis spectroscopy during the course of polymerization (Figure 2d-f and Supplementary Information) supports changes in reaction process. Polymerization was performed in diluted solution (1:10) to slow down the kinetics. Under these conditions, the polymerization of pure pyrrole takes at least 800 min until extinction of visible light strongly increases. During the polymerization of neat dopamine, extinction in the blue wavelength range commences quickly and gradually increases, confirming the red color observed optically and indicating activation upon addition of ammonium persulfate. In the mixed

sample PPy-DA_1, extinction pattern in the first minutes resembles the spectrum of dopamine polymerization but quickly and drastically increases over the whole wavelength range. Notably, the range of high extinction at higher energy (UV) expands to lower energy in the mixed polymer, indicating a change of the overall collective band structure and the band gap.[28] The mixed sample indeed polymerizes fastest and creates an electronically different species. The polymerization is boosted by the activated dopamine after addition of ammonium persulfate. Photographs of the reaction mixtures from Figure 2d-f after the polymerization (Figure S9) resemble the ones of Figure 2a-c.

Elemental analysis (Table 1) and thermographic analysis (Figure S10) confirm incorporation of both monomers into the final polymer. The composition of copolymers is between the one of pure polypyrrole (pyrrole C_4H_5N; theoretical C-to-N ratio 4:1) and pure polydopamine (dopamine $C_8H_{11}NO_2$; theoretical C-to-N ratio 8:1). Doping of the copolymers increases with increasing dopamine content as can be derived from increasing sulfur content (from sulfate counter ions). This already indicates a higher possible charge storage in the conjugated copolymer via a doping-undoping mechanism. Interestingly, the product from neat dopamine polymerization with APS as oxidant is different from the expected structure. A low carbon-to-nitrogen ratio does not agree with PDA, indicating side reactions during the polymerization of pure dopamine with APS. In contrast, self-polymerization of dopamine by stirring in air leads to a product with almost the expected carbon-to-nitrogen ratio (but not doped due to the absence of APS). Consequently, neither of the PDA materials is suited for comparison with PPy-Da_x polymers regarding their electric properties (see below). Thermal decomposition of PPy-DA_x samples (Figure S10) results in residual masses which are almost independent on the composition (PPy-$DA_{0.32}$ shows almost exactly the same decomposition behavior as PPy-DA_1). Pure polydopamine leaves less material behind after thermogravimetric analysis, and pure PPy results in higher residues. Temperatures at which decomposition commences are similar.

Table 1 Composition of the different samples (carbon, nitrogen, sulfur, and hydrogen content) as determined by elemental analysis.

Sample	C [%]	N [%]	S [%]	H [%]	C-to-N ratio
PPy	54.76	15.28	4.02	3.85	3.58
PPy-$DA_{0.16}$	53.82	13.59	5.81	4.38	3.96
PPy-$DA_{0.32}$	51.40	12.02	6.78	4.52	4.28
PPy-DA_1	51.41	11.63	7.19	4.65	4.42
PDA (with APS)	31.00	9.92	12.52	5.12	3.13
PDA (w/o APS)	55.75	7.56	0.83	4.68	7.38

3.2. Nanostructure Formation

In the following, we will elaborate on the interaction of both monomers during the polymerization as this will turn crucial for energy storage behavior (see below). Figure 3 shows SEM images of the fluffy product PPy, the fine powders obtained from copolymerized pyrrole-dopamine samples PPy-DA_x, or the freeze-dried product from the polymerization of dopamine (PDA), where the precipitate was too fine to separate. Polymers made from the neat monomers clearly differ from each other and from the mixed pyrrole-dopamine polymers. The freeze-dried product from neat dopamine polymerization has a platelet-like structure. In contrast, polypyrrole forms aggregated spherical particles several hundred nanometers in diameter. Addition of dopamine to the pyrrole polymerization leads to elongated aggregates or nanofibrilles with diameters less than 100 nm and different length, which are insoluble in every solvent investigated.

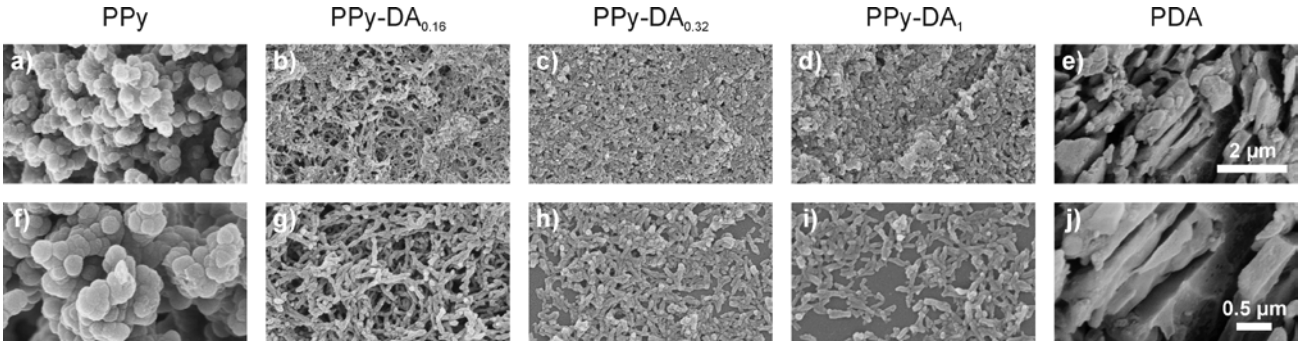

Fig. 3 SEM images of PPy (a,f), PPy-$DA_{0.16}$ (b,g), PPy-$DA_{0.32}$ (c,h), PPy-DA_1 (d,i), and PDA (e,j) after polymerization with different magnification. The scale bar in (e) corresponds to (a-e). The scale bar in (j) corresponds to (f-j).

In the case of different PPy-DA_x copolymers, the shape and length of nanofibrilles is independent on the monomer feeding ratio. Previous reports suggested that the fibrous morphology may be caused by sterical hindrance and increased hydrophilicity upon incorporation of dopamine into polypyrrole chains or structures in which polydopamine is coated onto a polypyrrole core.[21] However, a nanofibrille structure is uncommon for statistical amphiphilic copolymers.[29, 30]

A second possibility is the formation of a charge transfer complex of pyrrole and dopamine units. The interaction of the (hetero-)aromatic rings of pyrrole (electron-poor) and dopamine (electron-rich) has previously been presented as a reason for increased conductivity in PPy-DA copolymers. Also the oxidation potential of pyrrole significantly decreases upon addition of dopamine.[23] Formation of a charge transfer complex already between the monomers explains the increased polymerization rate of the monomer mixture and might also be responsible for nanofibrille structures. Scheme 1 illustrates a simplified model how it supports aggregation and condensation to one-dimensional structures.

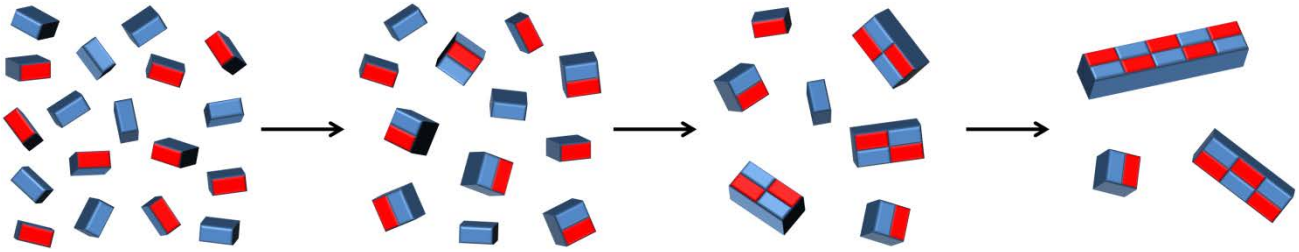

Scheme 1 Idealized schematic how the polymerization of dopamine (blue) with pyrrole (red) might proceed. A charge transfer complex between the monomers is formed first, leading to linear constraint growth into nanofibrilles. We note that different possible linkages of dopamine units exist, so only an idealized structure is shown.

Fourier Transform Infrared Spectroscopy (FT-IR) of the different polymers confirms the interactions of dopamine and pyrrole units in the polymer instead of a simple mixture of both monomers. Figure 4 summarizes the results. Enlarged spectra in the area of lower wavenumber than 1750 cm^{-1} are summarized in Figure S11 in the Supplementary Information. The spectra resemble previous reports, which however simply indicated that the IR spectrum of the copolymer "contains the characteristics of both pure PPy and PDA, supporting the observation that PDA has been successfully incorporated into the PPy network".[22] Changes of the copolymer spectrum compared to the homopolymer spectra were not discussed.

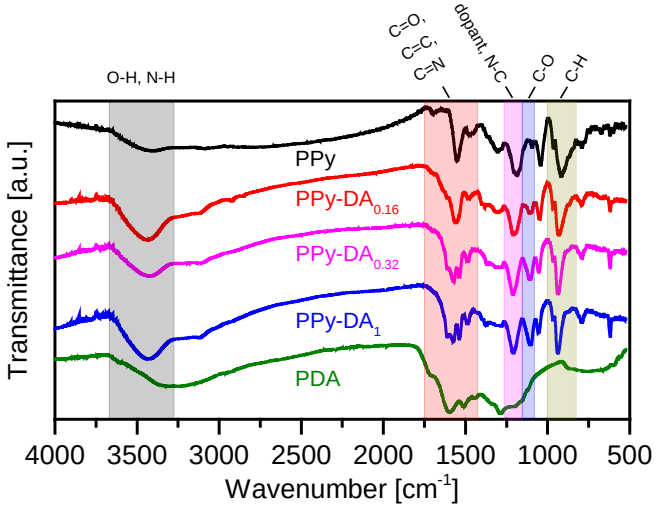

Fig. 4 FT-IR spectra of the individual samples as indicated.

Linkages in polydopamine are manifold;[16, 31] still the FT-IR spectrum clearly contains peaks denoting to O-H and N-H stretching vibrations (broad in the range of 3300 cm^{-1}), C=O and C-O stretching vibrations (1720 cm^{-1} and 1290 cm^{-1}, respectively) as well as C=C and C=N stretching vibrations in the aromatic ring (1600 cm^{-1} and 1510 cm^{-1}, respectively).[32, 33] Also the FT-IR spectrum of polypyrrole resembles reported spectra from the literature.[34]

C=C and C-N stretching vibrations of the ring are observable in the range of 1550 cm^{-1} and 1480 cm^{-1}, respectively as well as =C-H inplane vibrations around 1300 cm^{-1} and 1040 cm^{-1} and -C-H bending vibrations around 920 cm^{-1}.[34-36]

With increasing amount of dopamine incorporated throughout the polymerization, significant changes are observed in the area of C=C and C=N aromatic stretching vibrations (approx. 1500 cm^{-1} to 1600 cm^{-1}), in the shifting peak from 1190 cm^{-1} to 1210 cm^{-1} (dopant or N-C vibrations),[34, 37] in the increasing intensity around 1100 cm^{-1} (C-O or C=S, denoting to oxidation products or reactions with the dopant),[38] and in the shifting peak around 900 cm^{-1} to 940 cm^{-1} (C-H). Furthermore, peaks in the range of 2900 cm^{-1} indicate aliphatic C-H stretching vibrations,[33] which can best be observed for low dopamine-to-pyrrole ratio. The occurrence of these peaks indicates that cyclization of dopamine (cf. Figure 1) is incomplete in such samples.

Especially changes in the aromatic stretching vibrations are noteworthy. In this range, an additional peak around 1610 cm^{-1} increases in intensity with more dopamine in the sample, and the peak at 1550 cm^{-1} first broadens in PPy-$DA_{0.16}$ and splits up into two clearly separated peaks around 1575 cm^{-1} and 1535 cm^{-1} at higher concentrations of dopamine. This might indicate interaction of the two monomers in the polymer, shifts of electron density, formation of a charge transfer complex, a non-blocky structure, as well as carbonyl groups.

FT-IR spectra thereby confirm increased doping upon incorporation of dopamine into pyrrole and hence a decreased polaron delocalization length as well as interactions between the aromatic units of pyrrole and dopamine. While the structure of PPy-DA copolymers cannot completely be elucidated, all observations support strong interactions between pyrrole and dopamine (-derived) structural units. Polydopamine and polypyrrole do not form individual polymers which are mixed in the samples, but rather a copolymer. This influences charge storage as we will discuss next.

3.3. Energy Storage Performance

In the mixed PPy-DA_x polymers, electrical conductivity is highest for low dopamine-to-pyrrole ratios.[22] Compositions with equal amount of pyrrole and dopamine have a conductivity in the range of 1.5 mS cm^{-1}, while the conductivity of polypyrrole is in the range of 40 mS cm^{-1} (numbers for compressed pellets). The product from polymerization of dopamine under the same conditions is non-conductive.[21, 22] Even though electrical conductivity is lower than in samples with low amount of dopamine, more redox active quinone or hydroquinone functionalities are expected in polymers comprising large proportions of dopamine. For charge storage, both is important. Indeed, preliminary tests showed that highest capacity results for polymers that comprise an approximately 1:1 mixture of dopamine and pyrrole (PPy-DA_1), cf. Figure S12 in the Supplementary Information. In the following, we will hence present only the charge storage in PPy-DA_1.

Figure 5a shows cyclic voltammetry (CV) studies in a lithium cell setup. While the PPy-DA_1 voltammogram in the beginning resembles the one of pure polypyrrole (Figure S13 in the Supplementary Information), a characteristic broad peak around 3.0 V to 3.5 V vs. Li^+/Li

evolves after few cycles. Intensity of the peak region increases with prolonged cycling which makes sense given that during the redox reaction lithium phenolate is reversibly formed, and Li^+ cations as well as bulky PF_6^- anions and sulfate dopant move in and out of the electrode material, so structures need to rearrange for establishment of full charge storage. Hydroquinone functionalities, which are initially supposed to be present to some extent in polydopamine,[16] additionally first need to be deprotonated, and resulting reaction products need to be removed, e.g., by forming an SEI layer on the lithium anode. The peak region around 3.25 V vs. Li^+/Li is in the expected voltage range for quinones[10] and denotes to faradaic charge storage in the redox active polydopamine. In comparable polypyrrole samples, the overall current in CV curves also increases, however over a wider potential range and without such a clearly defined redox couple peak (Figure S13 in the Supplementary Information). The different development of the voltammograms indicates the influence of dopamine units on the charge storage and shows that they are only actively contributing after several charging-discharging cycles. We note that comparing the electrochemical behavior of PPy-DA_1 and PDA samples is not possible as neat dopamine, polymerized under the same conditions, does not form polydopamine (see above).

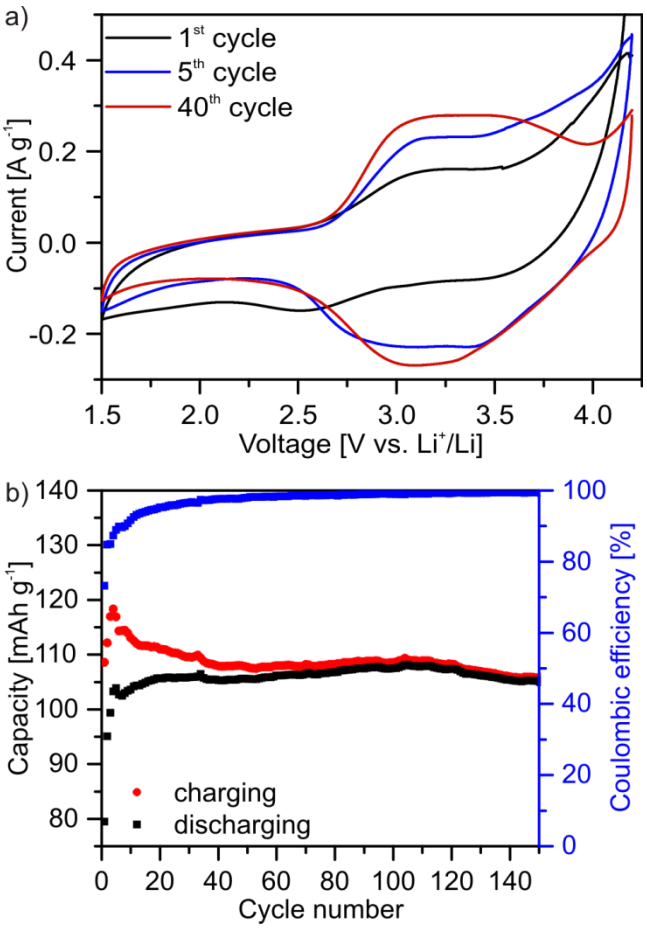

Fig. 5 a) Cyclic voltammetry of PPy-DA_1 at 1 mV s^{-1}. Selected cycles are displayed. b) Capacity of PPy-DA_1 samples as obtained from CV experiments . Coulombic efficiency (right axis of ordinates) as calculated from charging and discharging capacity (left axis of ordinates).

Integration of CV curves shows that over many cycles, around 105 mAh g^{-1} can be reversibly stored under these conditions with a high coulombic efficiency (Figure 5b). Initial mismatch between charging and discharging capacity is likely caused by side reactions with impurities and rearrangements of the structure. After this initial period, capacity is constant with a high coulombic efficiency.

At a specific current of 100 mA g^{-1} this results in a very favorable specific capacity of 155.7 mAh g^{-1} (or 1 electron per 172 mass units of organic matter; all specific data relative to the mass of active material). Compared to electrodes made from PPy (without incorporation of dopamine), this corresponds to an increase of approximately 25% (approximately 30 mAh g^{-1}) as shown in Figure 6. While there is only half as much pyrrole in PPy-DA_1 compared to PPy, doping is more pronounced (Table 1), so addition of DA lowers the polaron delocalization length in the conjugated polymer, enabling higher charge storage. In addition to this, quinone groups support additional faradaic charge storage in the copolymers. Combined, this amounts to approximately one electron per 0.95 dopamine molecules and one electron per 3.16 pyrrole molecules (assuming incorporation of dopamine and pyrrole monomers during the polymerization in the same 1:1 ratio as present in the reagent solution). Attribution of the stored electrons to the two processes is done also based on the evaluation of the kinetic behavior, as discussed next.

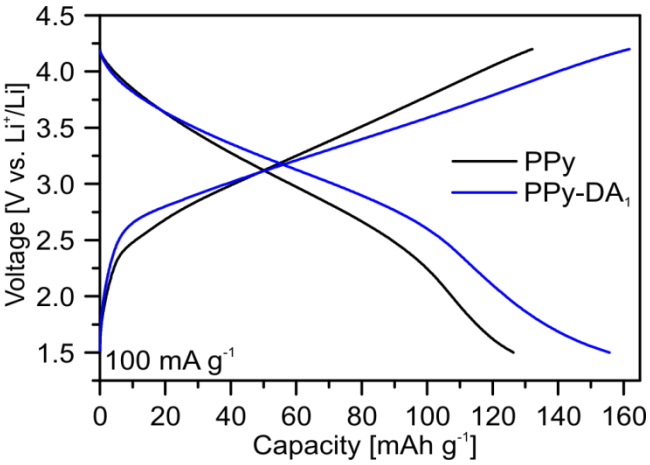

Fig. 6 Charging/discharging behavior of PPy-DA_1 and PPy electrodes at 100 mA g^{-1}.

The slopes of the discharging curves at a moderate rate of 100 mA g^{-1} illustrate the influence of polydopamine on charge storage: PPy discharging curves have an almost triangular shape as characteristic for charge storage in conjugated polymers. In contrast, the distinct redox reactions of the quinone groups in PPy-DA_1 result in additional charge storage around 3.25 V vs. Li^+/Li and hence a more belly-shaped discharging curve. This corresponds well to CV results in Figure 5a and Figure S13 in the Supplementary Information. Pure polypyrrole stores charges over a wider potential range as characteristic for a conductive polymer. Hence, during galvanostatic discharging, doped conjugated units are continuously reduced over a wide potential range and the full discharge cycle. Because of heavier doping, the

distance between localized charges in the conjugated backbone is shorter in copolymers, resulting in more continuous charge release from the conjugated backbone compared to pure polypyrrole. Quinone functionalities from dopamine units in the polymer are reduced more selectively at a narrower potential range around 3.25 V vs. Li^+/Li and hence more selectively early in the discharge cycle. Figure S14 in the Supplementary Information illustrates the sequence of reduction steps as derived from galvanostatic and cyclic voltammetry measurements (idealized model). During charging, galvanostatic experiments indicate continuous charge uptake over a wide potential range of approximately 2.5- 4.2 V vs. Li^+/Li and hence oxidation of the conjugated backbone and the phenolate units at the same time.

Discharging at different rate makes the belly shaped galvanostatic discharging curves even more obvious as illustrated in Figure 7a. Especially at high discharging rate (800 mA g^{-1}, corresponding to a complete discharge within 6.6 min), capacity mainly origins from the region between 2.5 and 3.5 V vs. Li^+/Li, in which quinones contribute to charge storage. Then still approx. 90 mAh g^{-1} are obtained, which we understand as a very favorable rate behavior. High capacity at fast cycling is usually obtained in surface confined redox reactions, with the migration of PF_6^- anions setting a limit to the capacity. Elongated structures of PPy-DA copolymers as observed in the SEM images (Figure 3) enable the good rate capability as they support exposure of functional groups to the electrolyte and a non-intercalation type charge storage. The rate capability calculated at different charging/discharging rates is summarized in Figure 7b. Capacity is constant within eleven charging-discharging events at a specific current. After multiple cycles at higher current, the initial discharging capacity is reached again, indicating that the electrodes are stable, and capacity is not fading within multiple cycling. The coulombic efficiency especially at slow discharge rate is however notably decreased. This may be attributed to side reactions which occur if not only surface confined functionalities contribute to charge storage. As noted above, in early charging-discharging cycles side reactions and structure rearrangements occur. If at slower discharging rate now more and harder accessible functional groups also contribute to charge storage this inherently results in more side reactions and explains the lower coulombic efficiency.

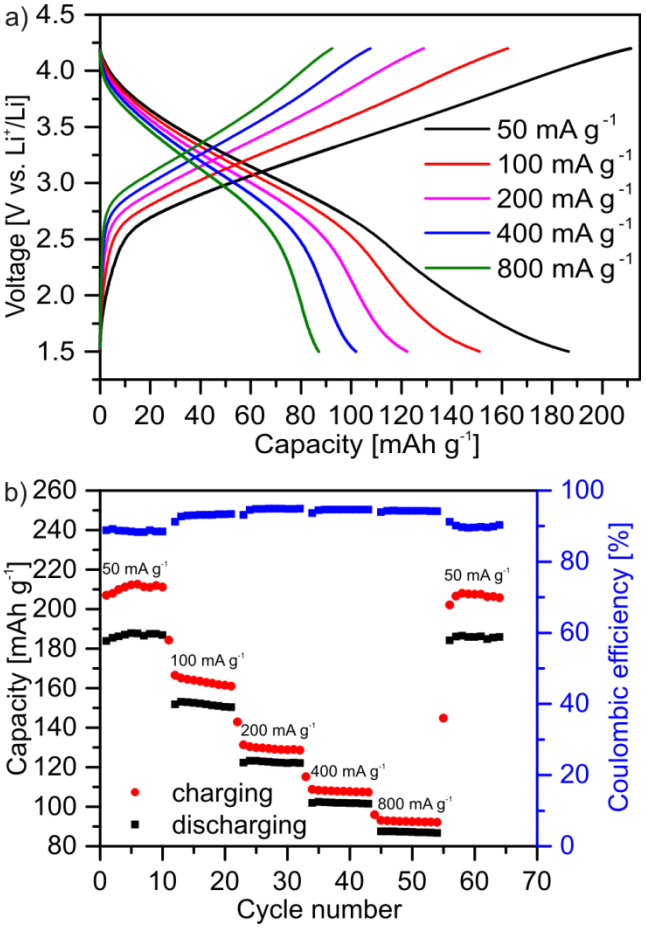

Fig. 7 . a) Rate dependence of the charging and discharging behavior illustrating capacity depending on the charging/discharging rate as indicated. b) Rate capability of PPy-DA_1 electrodes. Charging and discharging capacity in red and black, respectively, in dependence of the specific current are shown on the left axis of ordinates together with the coulombic efficiency (right axis of ordinates).

This is even more obvious when investigating battery cycling at constant charging-discharging rate. Figure 8 shows that upon 55 charging/discharging cycles at 100 mA g^{-1}, capacity is constant around 160 mAh g^{-1}, after an initial period in which discharging capacity slightly increases and charging capacity decreases. The coulombic efficiency continuously increases to more than 97 %. This demonstrates that electrodes do not decompose, and it takes several cycles for the quinone redox species to be fully active as also evidenced by cyclic voltammetry (Figure 5a) and discussed above.

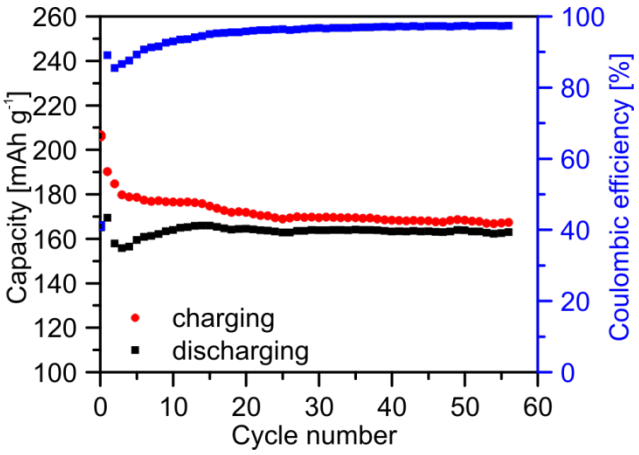

Fig. 8 Stability of PPy-DA_1 electrodes. Charging and discharging was performed at 100 mA g^{-1}. Coulombic efficiency (right axis of ordinates) as calculated from charging and discharging capacity (left axis of ordinates).

The charging and discharging curves resemble the ones obtained from integration of CV experiments (Figure 5b). In the first cycles significantly more charge is used for charging than available upon discharging. The difference is presumably used for activation of the system, deprotonation of remaining hydroquinones and/or formation of an SEI layer on the lithium counter electrode from reactions with impurities and traces of water. Constant capacity after some preconditioning cycles however demonstrates the formation of a stable redox active sustainable cathode material for future battery systems.

4. Conclusions

We emphasize that charge storage is a result of the mixed conjugated structure in which positively doped units as well as quinone groups are present. Furthermore, while oxidizing neat dopamine with ammonium persulfate leads to decomposition products, the presence of pyrrole moderates the reaction to result in the desired copolymer. The combination of both monomers is responsible for nanostructure formation during the synthesis, which in turn facilitates high charge storage when using the material as an effective and active cathode in a lithium cell setup. Charge storage in the range of 160 mAh g^{-1} at discharging rates of 100 mA g^{-1} compares already in this first set of experiments very nicely with the charge storage capacity of the common cathode material $Li_{0.5}CoO_2$ (approximately 150 mAh g^{-1}), however at a slightly lower voltage. This is worth underlining as the use of cobalt in cathodes for lithium based batteries can be as such avoided completely, while compromising energy density only weakly.

Even discharging at 800 mA g^{-1} results in approximately 90 mAh g^{-1}, which is rather high both for a polymer as well as an intercalation compounds. This speaks for an ion exchange on the surface of the as synthesized fibrous nanostructure rather than ion transport through a solid and is considered also very favorable for practical use. Batteries based on the biomolecule dopamine may hence be a good step towards more sustainable energy storage.

5. Acknowledgements

We highly appreciate help in the laboratory by Jessica Brandt. Philipp Adelhelm, Yusuf Yagci, and Jinyeon Hwang are acknowledged for constructive discussions. We are grateful for help with UV-Vis and TGA measurements by Antje Völkel, elemental analysis by Sylvia Pirok, SEM measurements by Heike Runge, and financial support by the Max Planck Society.

6. References

[1] L.A.-W. Ellingsen, G. Majeau-Bettez, B. Singh, A.K. Srivastava, L.O. Valøen, A.H. Strømman, Life Cycle Assessment of a Lithium-Ion Battery Vehicle Pack, J. Ind. Ecol. 18 (2014) 113-124.
[2] K. Richa, C.W. Babbitt, G. Gaustad, Eco-Efficiency Analysis of a Lithium-Ion Battery Waste Hierarchy Inspired by Circular Economy, J. Ind. Ecol. 21 (2017) 715-730.
[3] D. Larcher, J.M. Tarascon, Towards greener and more sustainable batteries for electrical energy storage, Nat. Chem. 7 (2015) 19-29.
[4] J. Deng, W.-B. Luo, S.-L. Chou, H.-K. Liu, S.-X. Dou, Sodium-Ion Batteries: From Academic Research to Practical Commercialization, Adv. Energy Mater. 8 (2017) 1701428.
[5] J. Muldoon, C.B. Bucur, T. Gregory, Fervent Hype behind Magnesium Batteries: An Open Call to Synthetic Chemists-Electrolytes and Cathodes Needed, Angew. Chem. Int. Ed. 56 (2017) 12064-12084.
[6] J. Qiu, M. Zhao, Q. Zhao, Y. Xu, L. Zhang, X. Lu, H. Xue, H. Pang, Aluminum-based materials for advanced battery systems, Sci. China Mater. 60 (2017) 577-607.
[7] K. Lei, F. Li, C. Mu, J. Wang, Q. Zhao, C. Chen, J. Chen, High K-storage performance based on the synergy of dipotassium terephthalate and ether-based electrolytes, Energy Environ. Sci. 10 (2017) 552-557.
[8] A. Rosenman, E. Markevich, G. Salitra, D. Aurbach, A. Garsuch, F.F. Chesneau, Review on Li-Sulfur Battery Systems: an Integral Perspective, Adv. Energy Mater. 5 (2015) 1500212.
[9] L. Li, Z.-w. Chang, X.-B. Zhang, Recent Progress on the Development of Metal-Air Batteries, Adv. Sustain. Sys. 1 (2017) 1700036.
[10] S. Muench, A. Wild, C. Friebe, B. Häupler, T. Janoschka, U.S. Schubert, Polymer-Based Organic Batteries, Chem. Rev. 116 (2016) 9438-9484.
[11] Z. Song, Y. Qian, X. Liu, T. Zhang, Y. Zhu, H. Yu, M. Otani, H. Zhou, A quinone-based oligomeric lithium salt for superior Li–organic batteries, Energy Environ. Sci. 7 (2014) 4077-4086.
[12] Z. Luo, L. Liu, J. Ning, K. Lei, Y. Lu, F. Li, J. Chen, A Microporous Covalent-Organic Framework with Abundant Accessible Carbonyl Groups for Lithium-Ion Batteries, Angew. Chem. Int. Ed. 57 (2018) 9443-9446.
[13] S. Chaleawlert-umpon, T. Berthold, X. Wang, M. Antonietti, C. Liedel, Kraft Lignin as Electrode Material for Sustainable Electrochemical Energy Storage, Adv. Mater. Interfaces 4 (2017) 1700698.
[14] S. Chaleawlert-umpon, C. Liedel, More sustainable energy storage: lignin based electrodes with glyoxal crosslinking, J. Mater. Chem. A, 5 (2017) 24344-24352.
[15] S. Admassie, F.N. Ajjan, A. Elfwing, O. Inganäs, Biopolymer hybrid electrodes for scalable electricity storage, Mater. Horiz. 3 (2016) 174-185.
[16] J. Liebscher, R. Mrówczyński, H.A. Scheidt, C. Filip, N.D. Hădade, R. Turcu, A. Bende, S. Beck, Structure of polydopamine: a never-ending story? Langmuir 29 (2013) 10539-10548.
[17] A. Banerjee, S. Supakar, R. Banerjee, Melanin from the nitrogen-fixing bacterium Azotobacter chroococcum: a spectroscopic characterization, PLoS One 9 (2014) e84574.
[18] T. Liu, K.C. Kim, B. Lee, Z. Chen, S. Noda, S.S. Jang, S.W. Lee, Self-polymerized dopamine as an organic cathode for Li- and Na-ion batteries, Energy Environ. Sci. 10 (2017) 205-215.
[19] R.R. Mercer, A.F. Hubbs, J.F. Scabilloni, L. Wang, L.A. Battelli, D. Schwegler-Berry, V. Castranova, D.W. Porter, Distribution and persistence of pleural penetrations by multi-walled carbon nanotubes, Part. Fibre Toxicol. 7 (2010) 28.
[20] G. Milczarek, O. Inganäs, Renewable cathode materials from biopolymer/conjugated polymer interpenetrating networks, Science, 335 (2012) 1468-1471.

[21] W. Zhang, Z. Pan, F.K. Yang, B. Zhao, A Facile In Situ Approach to Polypyrrole Functionalization Through Bioinspired Catechols, Adv. Funct. Mater. 25 (2015) 1588-1597.
[22] W. Zhang, F.K. Yang, Z. Pan, J. Zhang, B. Zhao, Bio-inspired dopamine functionalization of polypyrrole for improved adhesion and conductivity, Macromol. Rapid Commun. 35 (2014) 350-354.
[23] J. Tan, Z. Zhang, Y. He, Q. Yue, Z. Xie, H. Ji, Y. Sun, W. Shi, D. Ge, Electrochemical synthesis of conductive, superhydrophobic and adhesive polypyrrole-polydopamine nanowires, Synthetic Met. 234 (2017) 86-94.
[24] Z. Wang, L. Zhou, P. Yu, Y. Liu, J. Chen, J. Liao, W. Li, W. Chen, W. Zhou, X. Yi, K. Ouyang, Z. Zhou, G. Tan, C. Ning, Polydopamine-Assisted Electrochemical Fabrication of Polypyrrole Nanofibers on Bone Implants to Improve Bioactivity, Macromol. Mater. Eng. 301 (2016) 1288-1294.
[25] W. Zhang, Y. Zhou, K. Feng, J. Trinidad, A. Yu, B. Zhao, Morphologically Controlled Bioinspired Dopamine-Polypyrrole Nanostructures with Tunable Electrical Properties, Adv. Electron. Mater. 1 (2015) 1500205.
[26] J. Rawson, P.J. Angiolillo, M.J. Therien, Extreme electron polaron spatial delocalization in pi-conjugated materials, P. Natl. Acad. Sci. USA 112 (2015) 13779-13783.
[27] R. Steyrleuthner, Y. Zhang, L. Zhang, F. Kraffert, B.P. Cherniawski, R. Bittl, A.L. Briseno, J.L. Bredas, J. Behrends, Impact of morphology on polaron delocalization in a semicrystalline conjugated polymer, Phys. Chem. Chem. Phys. 19 (2017) 3627-3639.
[28] K. Müllen, W. Pisula, Donor-Acceptor Polymers, J. Am. Chem. Soc. 137 (2015) 9503-9505.
[29] Y. Hirai, T. Terashima, M. Takenaka, M. Sawamoto, Precision Self-Assembly of Amphiphilic Random Copolymers into Uniform and Self-Sorting Nanocompartments in Water, Macromolecules 49 (2016) 5084-5091.
[30] T.J. Neal, D.L. Beattie, S.J. Byard, G.N. Smith, M.W. Murray, N.S.J. Williams, S.N. Emmett, S.P. Armes, S.G. Spain, O.O. Mykhaylyk, Self-Assembly of Amphiphilic Statistical Copolymers and Their Aqueous Rheological Properties, Macromolecules 51 (2018) 1474-1487.
[31] D.R. Dreyer, D.J. Miller, B.D. Freeman, D.R. Paul, C.W. Bielawski, Perspectives on poly(dopamine), Chem. Sci. 4 (2013) 3796-3802.
[32] H. Luo, C. Gu, W. Zheng, F. Dai, X. Wang, Z. Zheng, Facile synthesis of novel size-controlled antibacterial hybrid spheres using silver nanoparticles loaded with poly-dopamine spheres, RSC Adv. 5 (2015) 13470-13477.
[33] R.A. Zangmeister, T.A. Morris, M.J. Tarlov, Characterization of polydopamine thin films deposited at short times by autoxidation of dopamine, Langmuir 29 (2013) 8619-8628.
[34] J.W. Kim, F. Liu, H.J. Choi, S.H. Hong, J. Joo, Intercalated polypyrrole/Na^{+}-montmorillonite nanocomposite via an inverted emulsion pathway method, Polymer 44 (2003) 289-293.
[35] M. Omastová, J. Pionteck, S. Košina, Preparation and characterization of electrically conductive polypropylene/polypyrrole composites, Eur. Polym. J. 32 (1996) 681-689.
[36] G. Lu, C. Li, G. Shi, Polypyrrole micro- and nanowires synthesized by electrochemical polymerization of pyrrole in the aqueous solutions of pyrenesulfonic acid, Polymer, 47 (2006) 1778-1784.
[37] C. Xu, J. Sun, L. Gao, Synthesis of novel hierarchical graphene/polypyrrole nanosheet composites and their superior electrochemical performance, J. Mater. Chem. 21 (2011) 11253-11258.
[38] M. Hesse, H. Meider, B. Zeeh, Spektroskopische Methoden In Der Organischen Chemie, 7th ed., Georg Thieme Verlag, Stuttgart, New York, 2005.

Supporting Information

Biobased Polymer Cathodes with Enhanced Charge Storage

Clemens Liedel, Xuewan Wang, and Markus Antonietti*

Department of Colloid Chemistry, Max Planck Institute of Colloids and Interfaces, Research Campus Golm, Am Mühlenberg 1, 14476 Potsdam, Germany

E-mail: Clemens.Liedel@mpikg.mpg.de

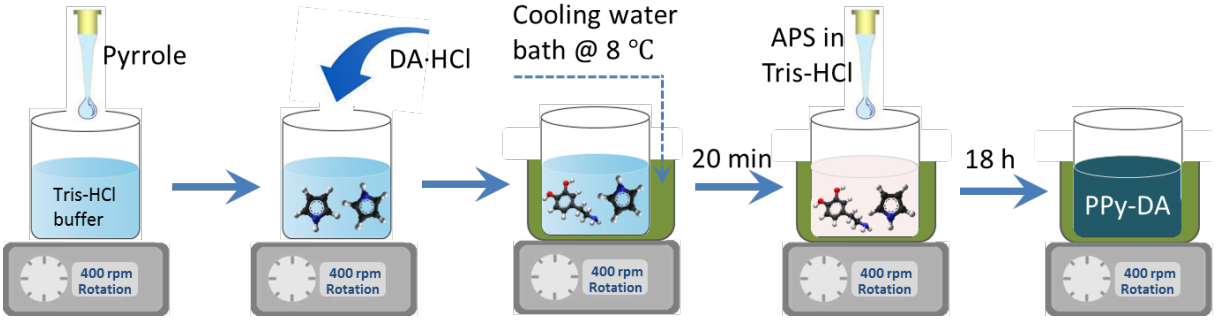

Figure S1: Schematic of the synthesis of PPy-DA samples.

Inside a UV-Vis spectrophotometer, we performed the synthesis under slightly modified conditions (samples were diluted 1:10 to better compare the kinetics and not stirred). Figure S2 compares selective specta. More spectra at different polymerization times are included in Figure S3 to Figure S8.

For polypyrrole, extinction independent on the wavelength in the visible range confirms the black sample color, probably caused by large conjugated π-systems and intermolecular interactions. In case of neat dopamine, extinction in the blue range immediately after addition of the oxidant confirms the red color observed in Figure 2c. With prolonged polymerization time, increasing extinction also in the near UV and violet range agrees with gradually changing color in Figure 2c. Obviously, the sample which includes both monomers polymerizes fastest, in accordance with observations in Figure 2b. Initially, the light absorption profile resembles the sample of neat dopamine, indicating that also here, dopamine is quickly activated by the oxidant. Already after few minutes, the sample becomes less

transparent with highest extinction coefficients at higher wavelength. The product has a different UV-Vis spectrum than either of the homopolymers or than the combination of both homopolymers, suggesting incorporation of both monomers in the final polymer structure as well as pronounced intermolecular charge transfer.

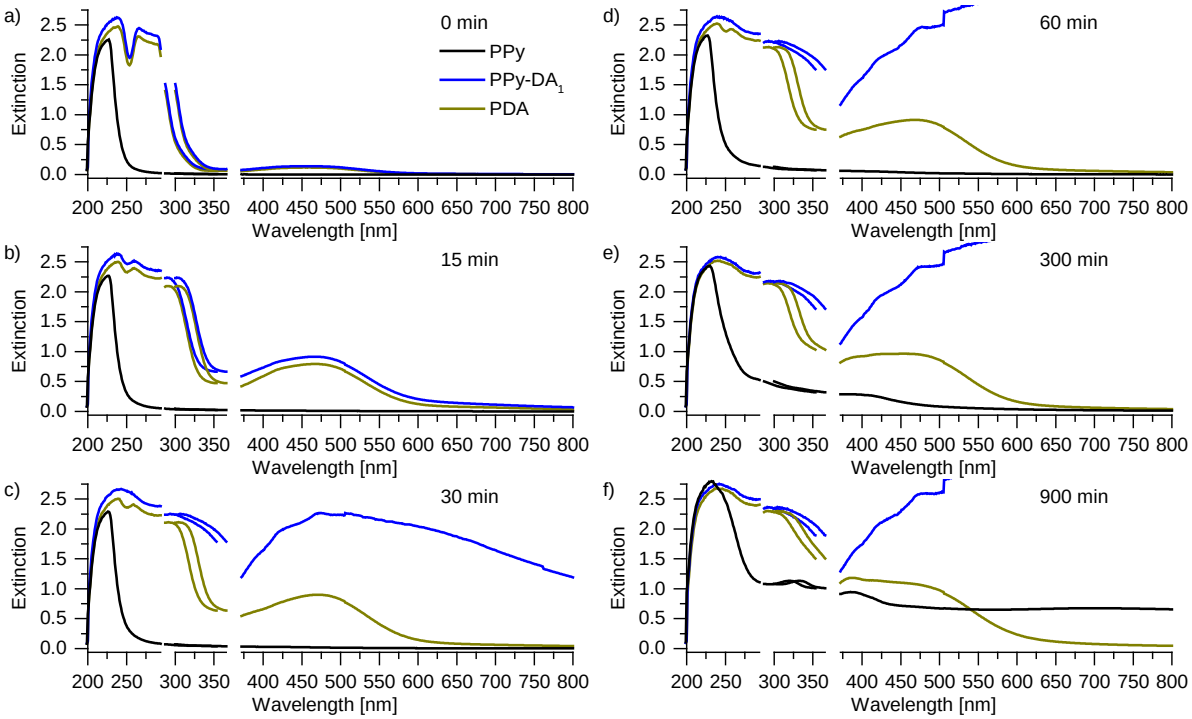

Figure S2: UV-Vis spectra of PPy, PPy-DA$_1$, and PDA after different polymerization times as indicated. Missing wavelengths are caused by different detectors and detector failures. The polymerization was performed in diluted solution (1:10) to slow down the kinetics.

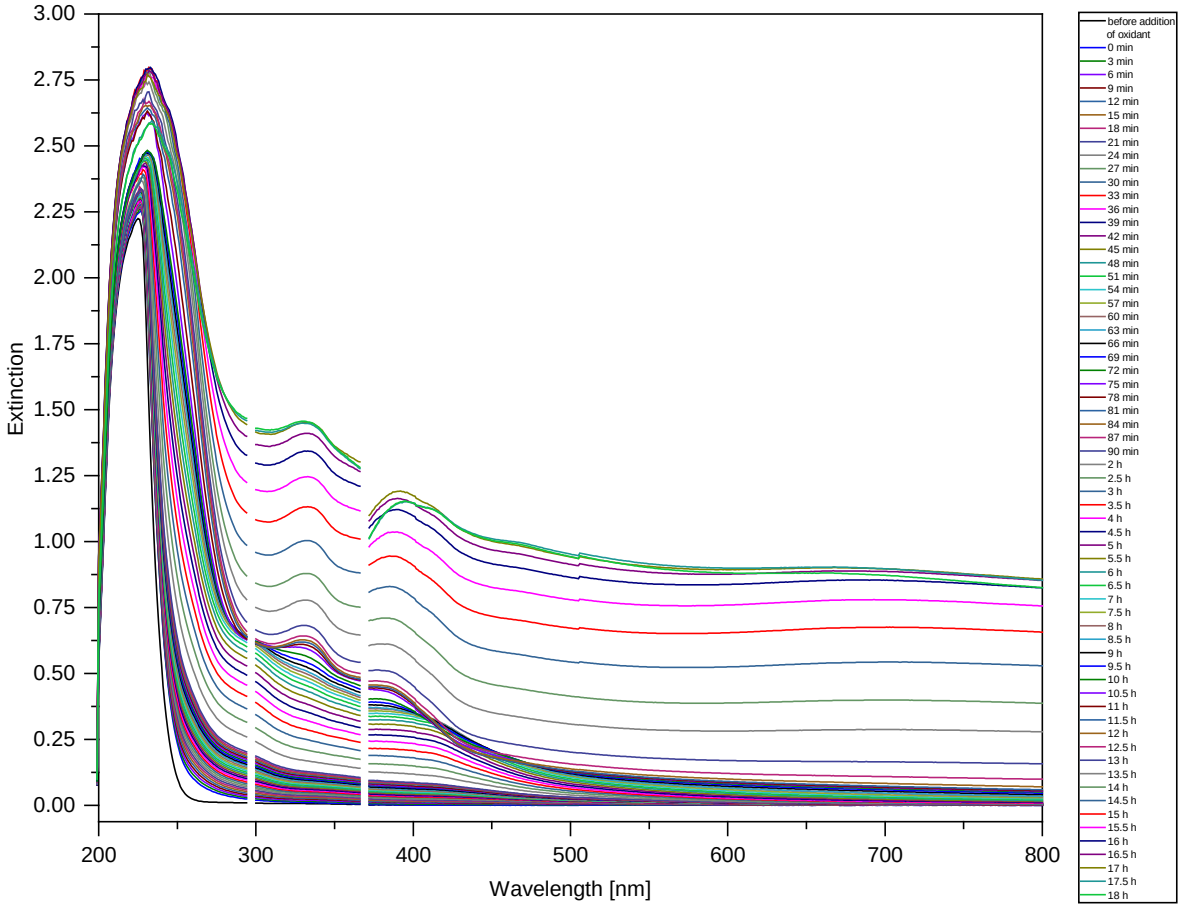

Figure S3: UV-Vis spectra during the polymerization of pyrrole with increasing polymerization times as indicated. Missing wavelengths are caused by different detectors and detector failures. The polymerization was performed in diluted solution (1:10) to slow down the kinetics.

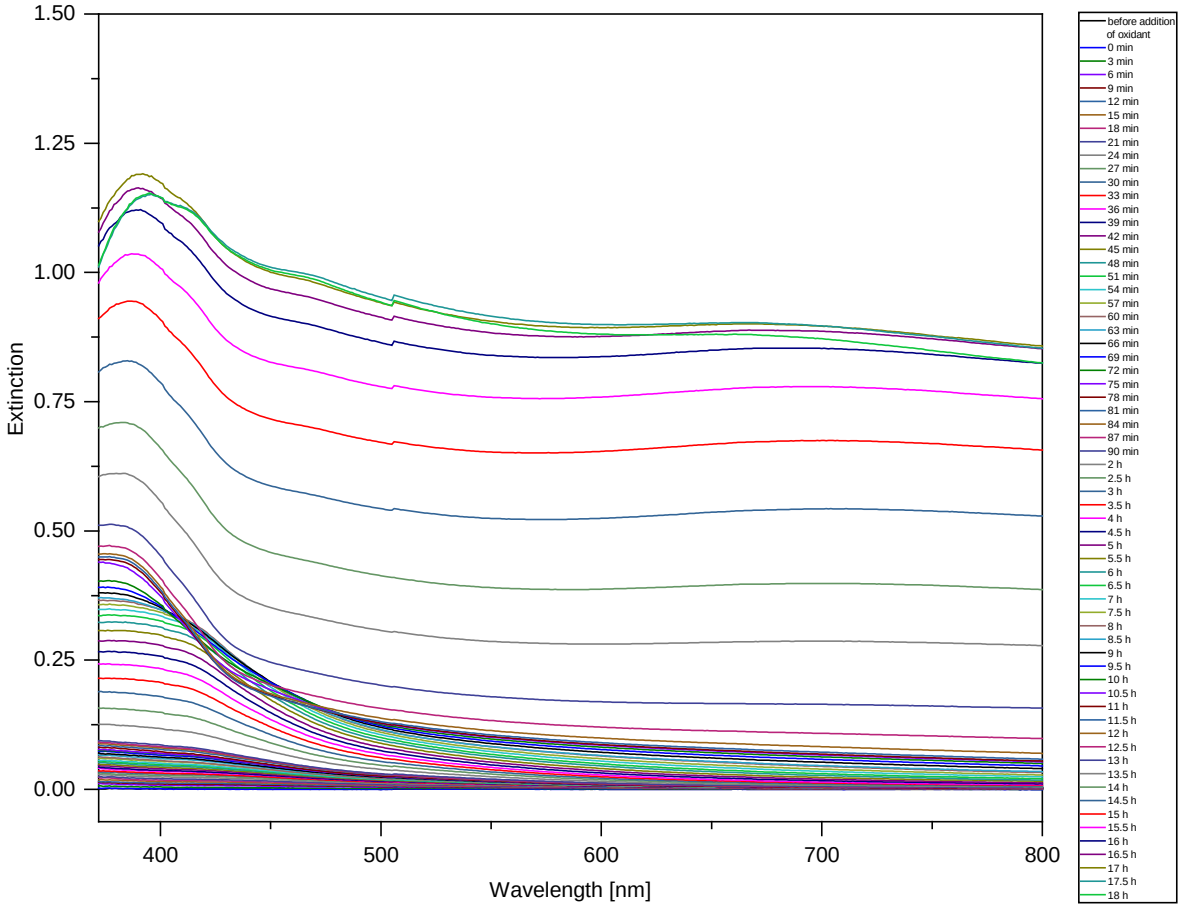

Figure S4: UV-Vis spectra (only the visible part of the spectra) during the polymerization of pyrrole with increasing polymerization times as indicated. Missing wavelengths are caused by different detectors and detector failures. The polymerization was performed in diluted solution (1:10) to slow down the kinetics.

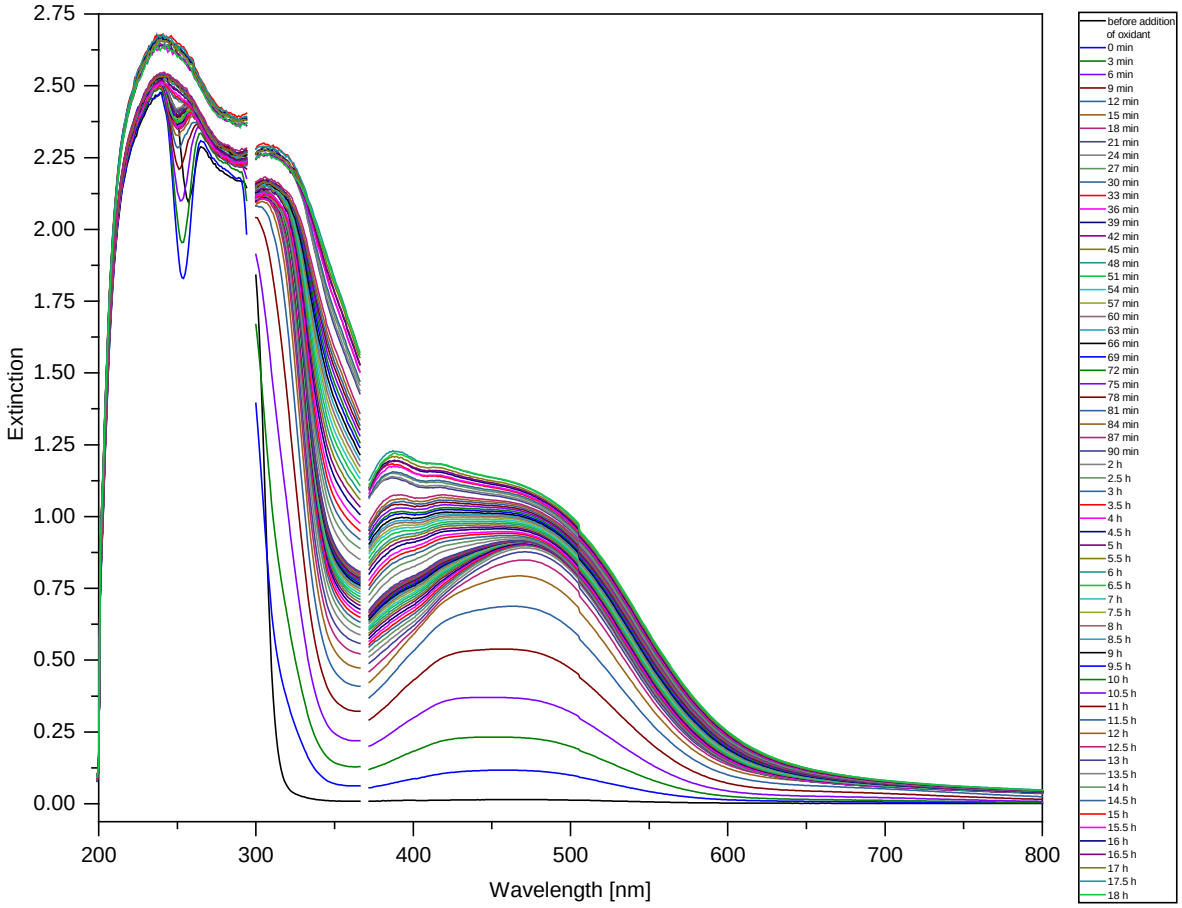

Figure S5: UV-Vis spectra during the polymerization of dopamine with increasing polymerization times as indicated. Missing wavelengths are caused by different detectors and detector failures. The polymerization was performed in diluted solution (1:10) to slow down the kinetics.

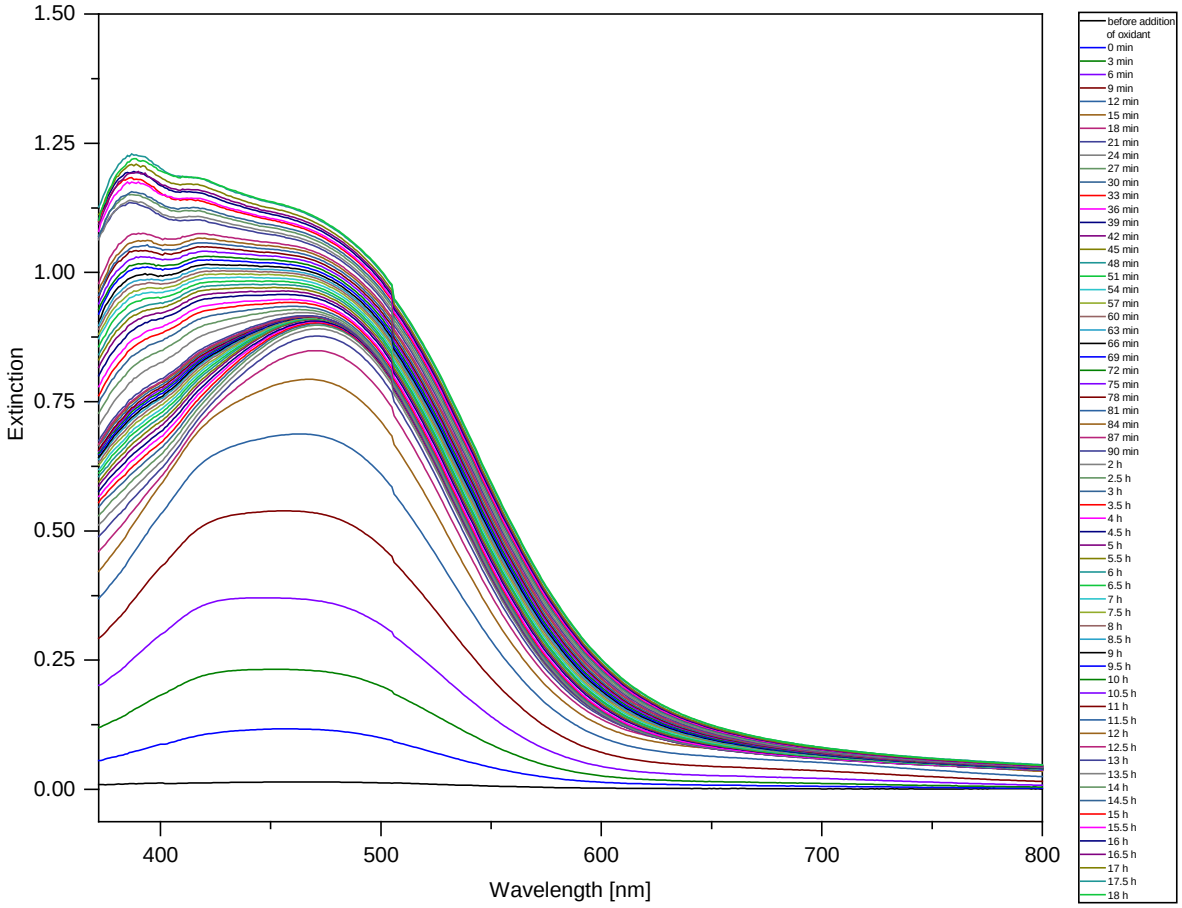

Figure S6: UV-Vis spectra (only the visible part of the spectra) during the polymerization of dopamine with increasing polymerization times as indicated. Missing wavelengths are caused by different detectors and detector failures. The polymerization was performed in diluted solution (1:10) to slow down the kinetics.

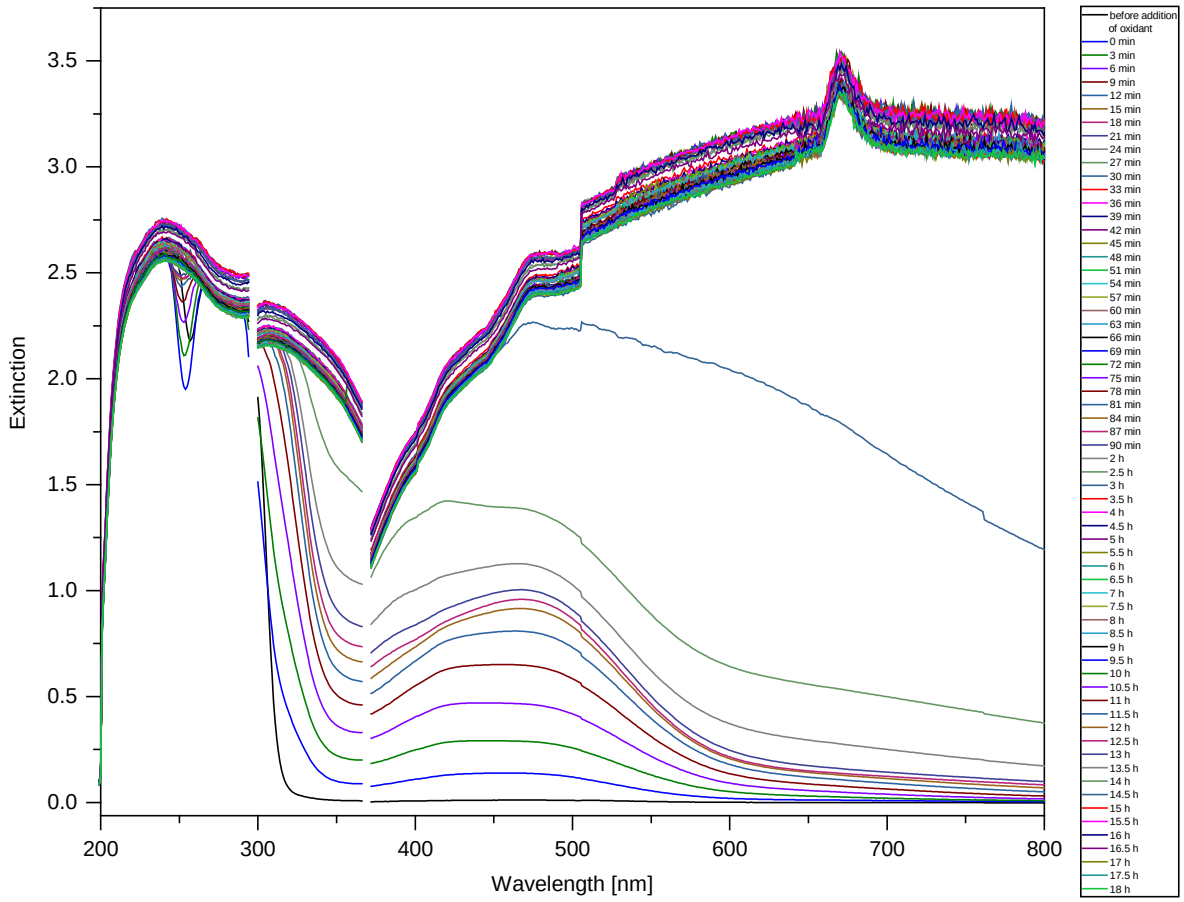

Figure S7: UV-Vis spectra during the polymerization of a 1:1 mixture of pyrrole and dopamine with increasing polymerization times as indicated. Missing wavelengths are caused by different detectors and detector failures. The polymerization was performed in diluted solution (1:10) to slow down the kinetics.

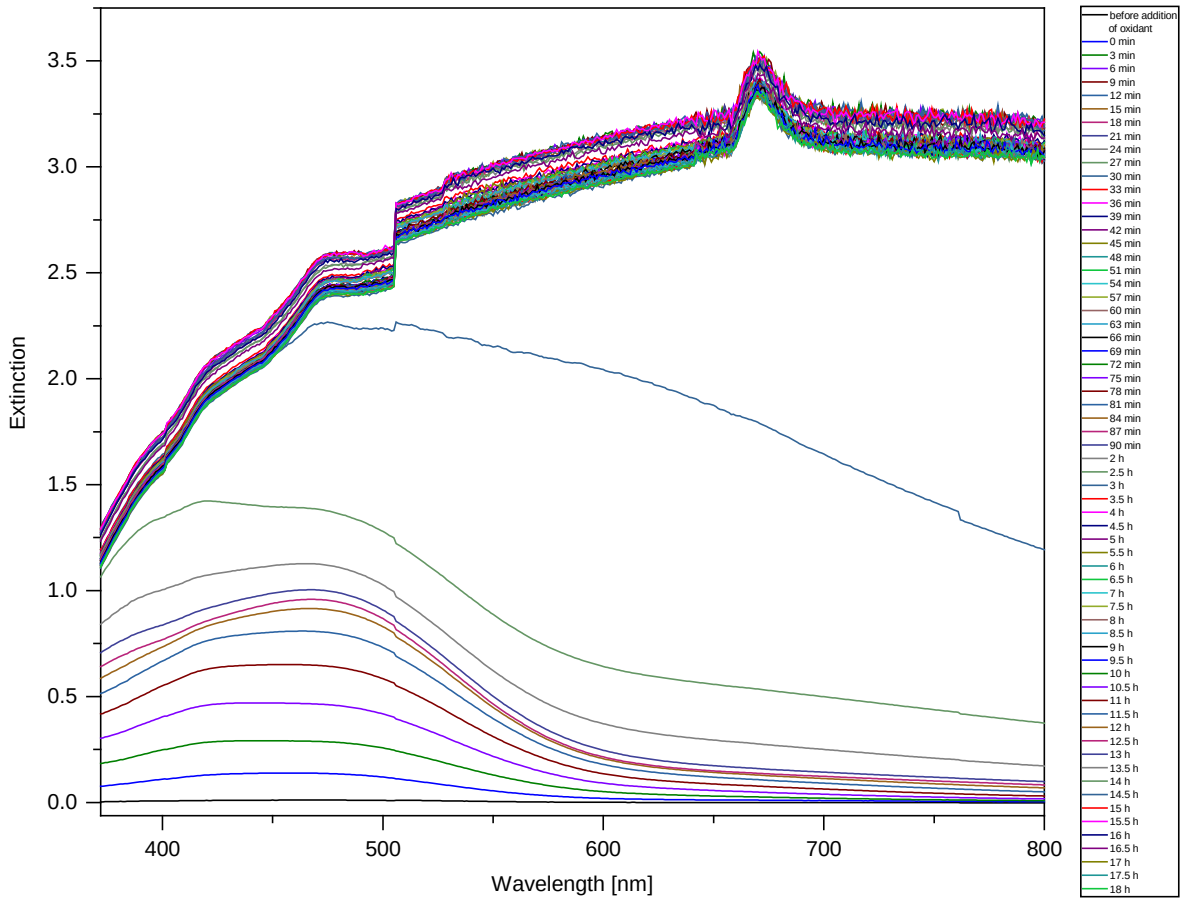

Figure S8: UV-Vis spectra (only the visible part of the spectra) during the polymerization of a 1:1 mixture of pyrrole and dopamine with increasing polymerization times as indicated. Missing wavelengths are caused by different detectors and detector failures. The polymerization was performed in diluted solution (1:10) to slow down the kinetics.

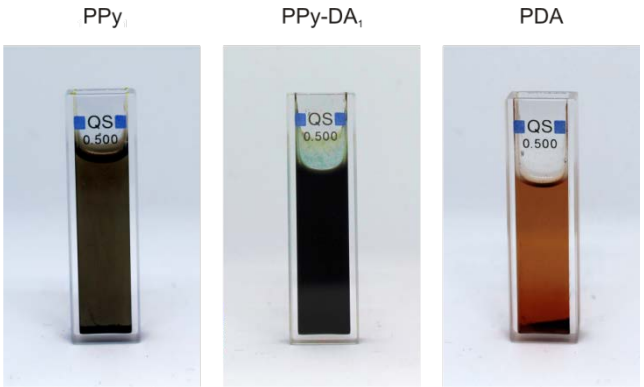

Figure S9: Photographs of samples as indicated after polymerization during UV-Vis measurements.

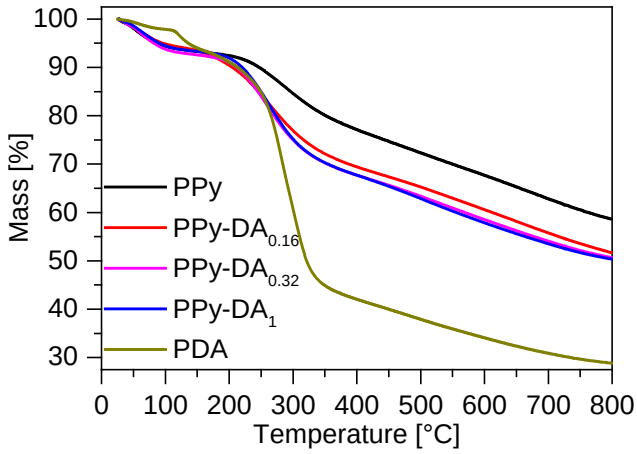

Figure S10: Thermogravimetric analysis plot of different samples as indicated.

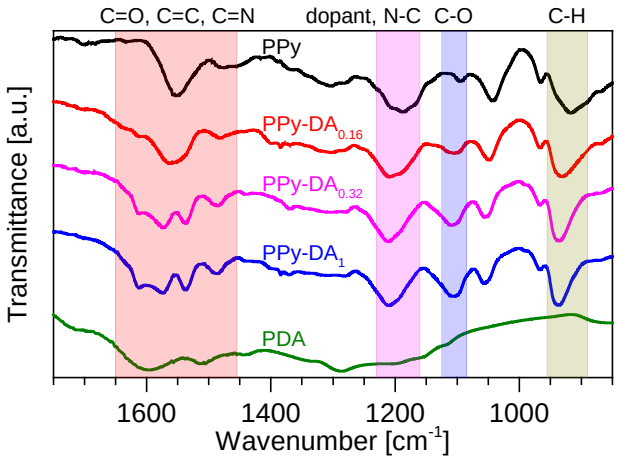

Figure S11: Fingerprint area of FT-IR spectra of the individual samples as indicated.

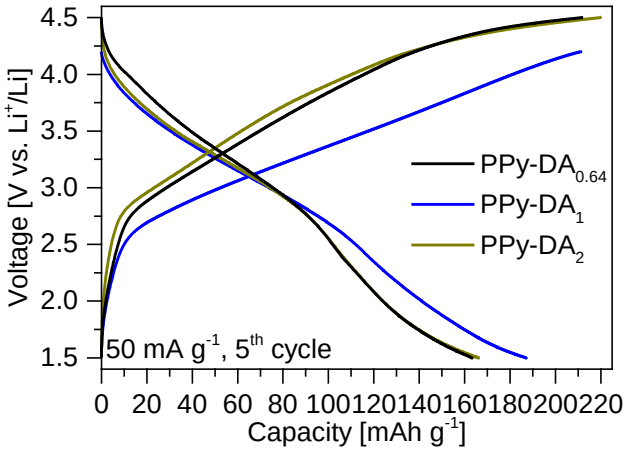

Figure S12: Capacity of PPy-DA$_x$ samples with different composition as indicated. Samples made with less dopamine than pyrrole (64%, black) and samples made with more dopamine than pyrrole (200%, green) have lower discharging capacity and lower coulombic efficiency compared to samples made from a 1:1 mixture of dopamine and pyrrole. For comparison, the fifth charging-discharging-cycle at 50 mA g^{-1} is shown.

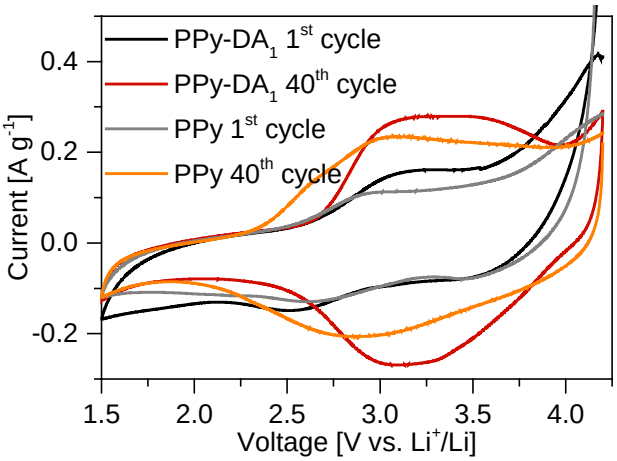

Figure S13: Comparison of cyclic voltammograms of PPY-DA$_1$ samples with PPy samples.

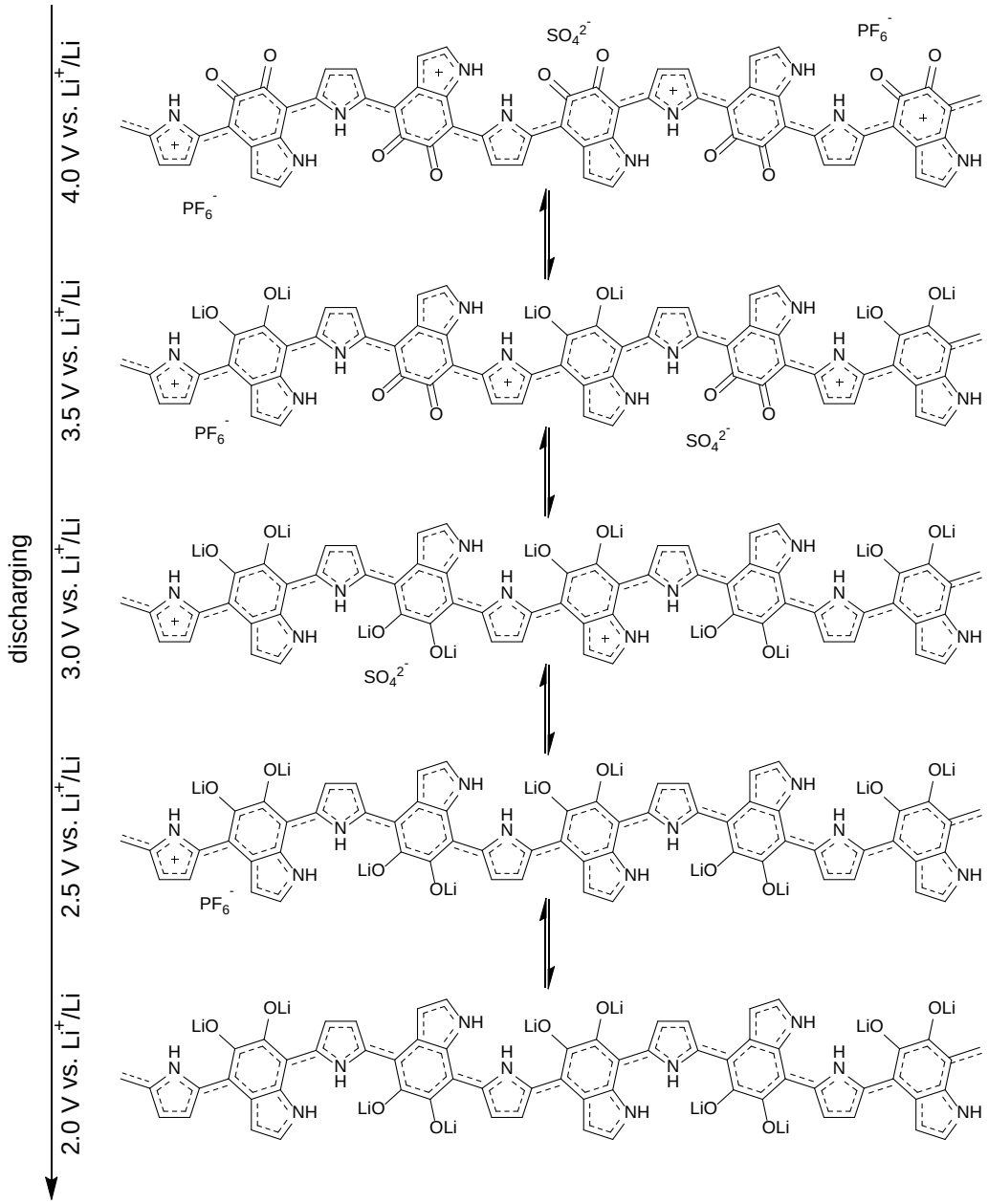

Figure S14: Schematic representation of the sequence of the electrochemical reduction process in galvanostatic discharging experiments. Idealized structures are shown, neglecting different monomer sequence and different monomer coupling in the polymer, as well as the fact that neither all quinone groups will be lithiated nor all doping reduced during discharging.